Impact of Nonlocal Electron Heat Transport on the High Temperature Plasmas of LHD

N. Tamura, S. Inagaki, T. Tokuzawa, K. Tanaka, C. Michael, T. Shimozuma, S. Kubo, K. Ida, K. Itoh, D. Kalinina, S. Sudo, Y. Nagayama, K. Kawahata, A. Komori and LHD team

National Institute for Fusion Science, 322-6 Oroshi, Toki, 509-5292, Japan

e-mail contact of main author: ntamura@LHD.nifs.ac.jp

Abstract. Edge cooling experiments with a tracer-encapsulated solid pellet in the Large Helical Device (LHD) show a significant rise of core electron temperature (the maximum rise is around 1 keV) as well as in many tokamaks. This experimental result indicates the possible presence of the nonlocality of electron heat transport in plasmas where turbulence as a cause of anomalous transport is dominated. The nonlocal electron temperature rise in the LHD takes place in almost the same parametric domain (e.g. in a low density) as in the tokamaks. Meanwhile, the experimental results of LHD show some new aspects of nonlocal electron temperature rise, for example the delay of the nonlocal rise of core electron temperature relative to the pellet penetration time increases with the increase in collisionality in the core plasma and the decrease in electron temperature gradient scale length in the outer region of the plasma.

1. Introduction

The definitive understanding of electron heat transport in magnetically confined plasmas is still an important issue, since the performance of a probable fusion reactor should be determined by electron heating as a result of the interaction between electrons and alpha particles as a fusion reaction product. In order to promote a better understanding of the electron heat transport, the electron heat transport analysis using a transient response has been carried out diligently in many tokamaks [1, 2] and helical systems [3, 4]. One of the significant issues found in these studies is a "nonlocal transport phenomenon" observed in perturbation experiments on many tokamaks [e.g. ref. 5] and a few helical systems [3] In particular, a rise of the core electron temperature T_e invoked by the rapid cooling of the edge plasma has been observed in various tokamaks with both ohmically heated plasmas and plasmas with an auxiliary heating, such as electron cyclotron heating (ECH), at a sufficiently low density. The amplitude reversal of the cold pulse propagation in the core plasma cannot be explained even by the local model based on the assumption that heat flux has a very strong nonlinear dependence on temperature and its gradient. In addition there seem to be no changes in the thermodynamic forces, such as those due to the temperature gradient and/or the density gradient, in the core plasma at the onset of the core T_e rise. Consequently, the core T_e rise invoked by the rapid edge cooling is considered to result from a nonlocality in the electron heat transport. Recently, to rationalize the so-called "nonlocal" T_e rise, some physics-based transport models including a critical gradient scale length, such as the ion temperature gradient (ITG) model, have been set up and tested [6]. It should be noted here that despite being dependent on local variables, the ITG-based model shows a nonlocal response to small changes in the profiles as a result of a slight deviation from near marginality. The ITG-based model with strongest stiffness can reproduce some of the same qualitative characteristics observed in carbon laser blow-off experiments in the TEXT tokamak. The magnitude and response time of the core T_e rise, however, is still in quantitative disagreement with those predicted by the strongest stiff ITG-based model. Moreover, it is an open question whether such models, which take into account two coupled heat diffusion equations (for ion and electron) with nonlinear thresholds and couplings, can be applied to the thermally decoupled electron-ion regime where the nonlocal T_e rise is mainly observed or not. In order to establish

a convincing theoretical reconstruction of the core T_e rise due to the nonlocal effect, a further experimental investigation in extensive parametric space into the cause and effect of the nonlocal T_e rise is required. More recently such a core T_e rise in response to the edge cooling is observed in a helical plasma [7]. The nonlocal T_e rise in helical device would contribute significantly, since helical systems have a quite different magnetic configuration (normally negative magnetic shear) and do not show a tokamak-like stiffness in the T_e profile [8]. In this paper, the experimentally-observed characteristics of nonlocal T_e rise invoked by the rapid edge cooling in a helical plasma are described.

2. Nonlocal Electron Temperature Rise in the LHD

Figure 1 shows a typical result of the peripheral cooling experiment in the LHD (major radius at the magnetic axis, R_{ax} = 3.5 m, an average minor radius, a = 0.58 m, magnetic field at the axis, B_{ax} = 2.829 T) by a tracer-encapsulated solid pellet (TESPEL [9]) injection. The TESPEL penetrated into the LHD plasma ablates typically less than ~ 1 ms and brings an increase in density and a decrease in temperature locally. In this discharge, the TESPEL penetration depth is ρ ~ 0.85. As can be immediately recognized in FIG. 1(a), a significant rise of the core T_e takes place in response to the edge cooling induced by the TESPEL injection. During the rising phase of the core T_e, neither density peaking (see FIG. 1(b)) nor significant change in low-m MHD modes are observed. As shown in FIG. 1(a), the discrepancy between the T_e measured and that simulated, which is obtained by solving the perturbed heat transport equation with a simple diffusion model [10], is quite noticeable in the core (ρ < 0.6) region. Meanwhile, the T_e behavior on the outside (ρ > 0.6) of the plasma shows a good agreement with the diffusion model. The LHD experiments on low-power NBI-heated plasmas (The magnetic configuration is the same as that in the discharge shown in FIG. 1, but the nonlocal T_e rise does not appear.) shows a weak dependence of the electron thermal diffusivity χ_e on the electron temperature gradient ∇T_e and a strong dependence (gyro-Bohm like, power = 3/2 ~ 5/2) of that on T_e [4]. The temporal evolutions of χ_e^{gB}, which is defined as $\chi_e^{gB}(\rho, t) = c(\rho)\chi_e^{PB}(\rho, t = 2.79\ \mathrm{s})T_e(\rho, t)^{3/2}$, to be expected from the result of the low-power NBI-heated LHD plasmas are shown in FIG. 1(c) with broken lines at three different normalized minor radii. Here, $\chi_e^{PB}(\rho, t = 2.79\ \mathrm{s})$ is the electron thermal diffusivity estimated by the power balance analysis at t = 2.79 s. The χ_e^{PB} around the

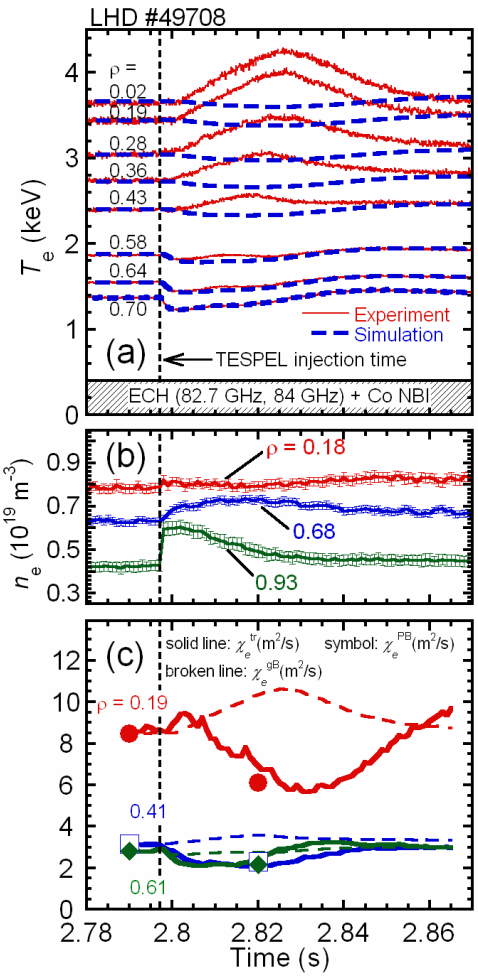

FIG. 1. Temporal evolutions of (a) the electron temperature measured (solid line) with the ECE radiometer at different normalized minor radii, (b) the electron density measured with the FIR interferometer at three different normalized minor radii. (c) Temporal evolutions of the electron thermal diffusivity to be expected from a gyro-Bohm like dependence ($\chi_e \propto T_e^{3/2}$) χ_e^{gB} (broken lines), that estimated by the power balance χ_e^{PB} (symbols), and that evaluated by the transient response analysis χ_e^{tr} (solid lines), at three different normalized minor radii. In (a) the simulated electron temperature (broken line) is also plotted. The TESPEL injection time is indicated as the vertical dashed line.

maximum of core T_e (t = 2.82 s) is, however, quite far from the χ_e^{gB} to be expected, and that is decreased by ~30 % compared to that before the edge cooling (t = 2.79 s), as seen in FIG. 1(c). The electron thermal diffusivity estimated by the transient response analysis χ_e^{tr} (= $-(q_{e0}+\delta q_e)/n_e\nabla(T_{e0}+\delta T_e)$) almost agrees with the χ_e^{PB}. (Details of the transient response analysis will be described in Section 4.) Here, q_{e0}, n_e, T_{e0} are the steady-state values before the TESPEL injection, and δq_e and δT_e are the electron heat flux perturbation and electron temperature perturbation, respectively. This indicates that there is validity of the estimate of electron heat flux perturbation by the transient response analysis. At ρ = 0.19, the χ_e^{tr} decreases and then increases gradually after the edge cooling. At ρ = 0.61, meanwhile, the χ_e^{tr} decrease abruptly then increases gradually after the edge cooling. The decreased χ_e^{tr} finally goes back to the level before the edge cooling, even with the constant heating power.

Within the time displayed in FIG. 1, the plasma is heated continuously by NBI in the co-direction (injected power ~ 2 MW) and ECH (injected power ~ 1 MW). The power of the neutral beam mainly goes into the electrons due to its high acceleration energy (~ 140 keV). Therefore the electron heat transport is the dominant thermal loss channel. Just before the TESPEL injection, the experimental energy confinement time τ_E^{exp} and electron-ion equipartition time τ_{ei} is ~ 50 ms and ~ 180ms, respectively. This condition allows the electron temperature to be inevitably higher than the ion temperature.

3. Characteristics of Nonlocal T_e Rise in LHD plasmas

In the LHD, the nonlocal T_e rise is observed in various plasmas. For example, the observation of nonlocal T_e rise in a plasma heated only with ECH (i.e. in a net-current free plasma) can completely rule out the contribution of the toroidal plasma current and the high-energy ions as a cause for the nonlocal T_e rise. In addition even a purely NBI-heated plasma shows the nonlocal T_e rise. Therefore the high-energy electrons also cannot lead to the nonlocal T_e rise.

Figure 2 shows a dependence of the peak electron temperature after the edge cooling normalized by the electron temperature just before the edge cooling $\delta T_{e(peak)}/T_e$ on the line-averaged electron density n_{e_bar} with various heating conditions, such as Co-, Counter(Ctr)-NBI overlapped with ECH and pure ECH. All the data in the FIG. 2 are summarized at ρ ~ 0.11. The positive value of the $\delta T_{e(peak)}/T_e$ indicates the increase of the T_e. The positive $\delta T_{e(peak)}/T_e$ become appreciable when the n_{e_bar} < 1.2 x 10^{19} m^{-3}. Above n_{e_bar} ~ 2.0 x 10^{19} m^{-3}, a significant positive $\delta T_{e(peak)}/T_e$, that is, the core T_e rise in response to the edge cooling is no longer observed. This inverse relationship between the nonlocal T_e rise and the electron density is also observed in many tokamaks. The empirical condition $n_e(0)/T_e(0)^{1/2}$ < 0.035 x 10^{19} $m^{-3}/eV^{1/2}$, which has been obtained in Ohmic plasmas in the TFTR, can predict the threshold for the appearance of the nonlocal T_e rise obtained in the LHD.

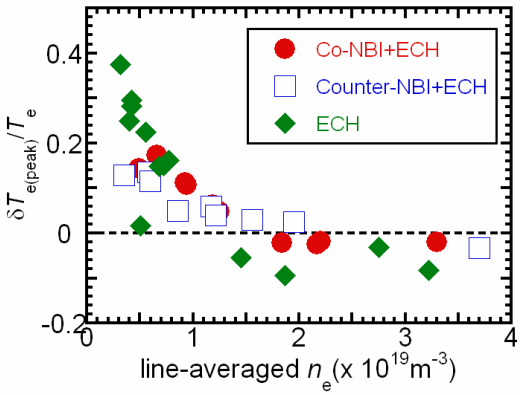

FIG. 2. The peak electron temperature after the edge cooling normalized by the electron temperature just before the edge cooling as a function of the line-averaged electron density in plasmas under various heating conditions.

A perceivable delay in the increase of the core T_e after the edge cooling is observed in many tokamaks [e.g., ref. 11]. Also in the LHD, it is observed such a delay until the T_e rise over the level just before the edge cooling, as shown in FIG. 3. When the n_e increases, the delay of the core T_e

rise becomes longer (In the case of FIG. 3, at ρ = 0.11, ~ 5 ms delayed at the n_{e_bar} with 0.94 x 10^{19} m^{-3}.), although the delay of the nonlocal T_e rise in the RTP tokamak is not increased with increase in the electron density [11]. It should be noted here that even with a delayed onset time of nonlocal T_e rise, the time of the T_e rise in the core region (ρ < 0.4) still has kind of a spatial uniformity. Figure 4(a) shows the delay in the T_e rise at $\rho = 0.11$ as a function of collisionality ν_b^*, which is electron collisionality obtained at $\rho = 0.11$ normalized by bounce frequency of banana orbit. The low collisionality ($\nu_b^* < 0.3$) is favorable for an instant nonlocal effect producing. In the high collisionality regime ($\nu_b^* > 3$), the nonlocal T_e rise is never observed. The direction of NBI seems not to cause much difference to the delay of the nonlocal T_e rise. (The main reason for the slight difference between the Co-NBI+ECH and the Ctr-NBI+ECH is due to the difference of the base transport caused by the NBI direction.) Figure 4(b) shows a dependence of the delay at $\rho = 0.11$ on the equivalent to the electron temperature gradient scale length at the peripheral region, $\rho = 0.58 \sim 0.78$. In FIG. 4(b), the ECE data, where the line-averaged electron density is less than 0.4 x 10^{19} m^{-3}, is not used for the analysis, since the high-energy electrons, which can appear in the plasma with such a low density, could affect the ECE signals. The delay of the onset of the core T_e rise increases with the decrease in the electron temperature gradient scale length at the peripheral region. This indicates that there exists critical electron temperature gradient scale length for the onset of the nonlocal T_e rise.

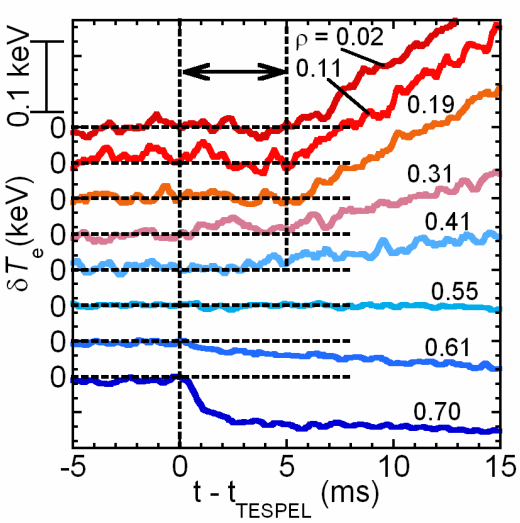

FIG. 3. Temporal evolution of perturbed electron temperature in a high electron density with the value of the line-averaged electron density, ~ 0.94 x 10^{19} m^{-3}. About 5 ms delay of the onset of the T_e rise is observed at $\rho = 0.11$.

The nonlocal T_e rise in the LHD plasmas is observed also when a small solid hydrogen pellet is injected as well as in tokamaks. Therefore the impurity seeding effect, such as radiative improved mode can be excluded as a reason of the nonlocal T_e rise in the LHD plasmas. The similarities in the nonlocal T_e rise between tokamaks and LHD suggest that the sign of the magnetic shear does not play an important role in this phenomenon. The comparison between the LHD and the W7-AS stellarator, in which the core T_e rise in response to the edge cooling

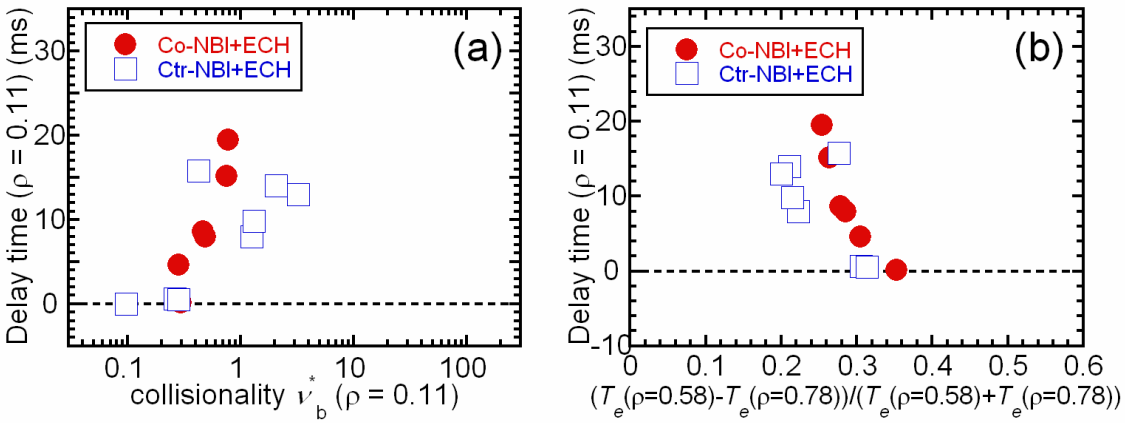

FIG. 4. Dependence of the delay until the T_e rise over the level just before the TESPEL injection at $\rho = 0.11$ on (a) the collisionality ν_b^*, and (b) the equivalent to the electron temperature scale length at the peripheral region $\rho = 0.58 \sim 0.78$.

has not been observed [12] indicates that the magnetic shear itself and/or the existence of the rational values of the rotational transform at the edge region could be a crucial part of the nonlocal T_e rise. Further investigation and experiments on this matter are necessary to conclude such a possibility.

4. Transient Response Analysis for the Plasma with the Nonlocal T_e Rise

The knowledge of the electron heat transport cannot be improved only by the power balance analysis, since it is based on the presumption that the local heat flux is proportional to the local ∇T_e. The detailed study of flux-gradient relation is essential to determine whether there is a "nonlocality" in the transport. In order to examine in-depth the dynamic behavior of the electron heat transport during the core T_e rise, a transient response analysis is carried out around the time of the edge cooling. The perturbed equations for the conservation of energy and particles are given by ref. [1]. The electron heat flux perturbation δq_e can be evaluated by deforming the energy conservation equation for the electron perturbation,

$$\delta q_e(r,t) = -\frac{1}{r}\int_0^r \frac{3}{2} n_e \frac{\partial \delta T_e(r,t)}{\partial t} \rho d\rho. \qquad (1)$$

In arriving at the above equation, the terms related to the perturbation of n_e and the perturbed source terms of the heat and particles are ignored for the core region ($\rho < 0.6$), where is far from the region invaded by the TESPEL. Indeed, the experiment results show that n_e in the core region almost remains the same just before and after the TESPEL injection considering the accuracy of the Abel inversion technique as seen in FIG. 1 (b). In addition, the particle diffusivity, which is evaluated by the gas-puff modulation experiments, is much smaller than the thermal diffusivity [13]. Figure 5 shows the relation of the electron heat flux perturbation normalized by the electron density $\delta q_e/n_e$ to the electron temperature perturbation δT_e and the gradient of that $\nabla \delta T_e$ at three different normalized minor radii for the discharge shown in FIG. 1. In FIG. 5, the data points obtained at 1 ms intervals are started from t = 2.798 s. The

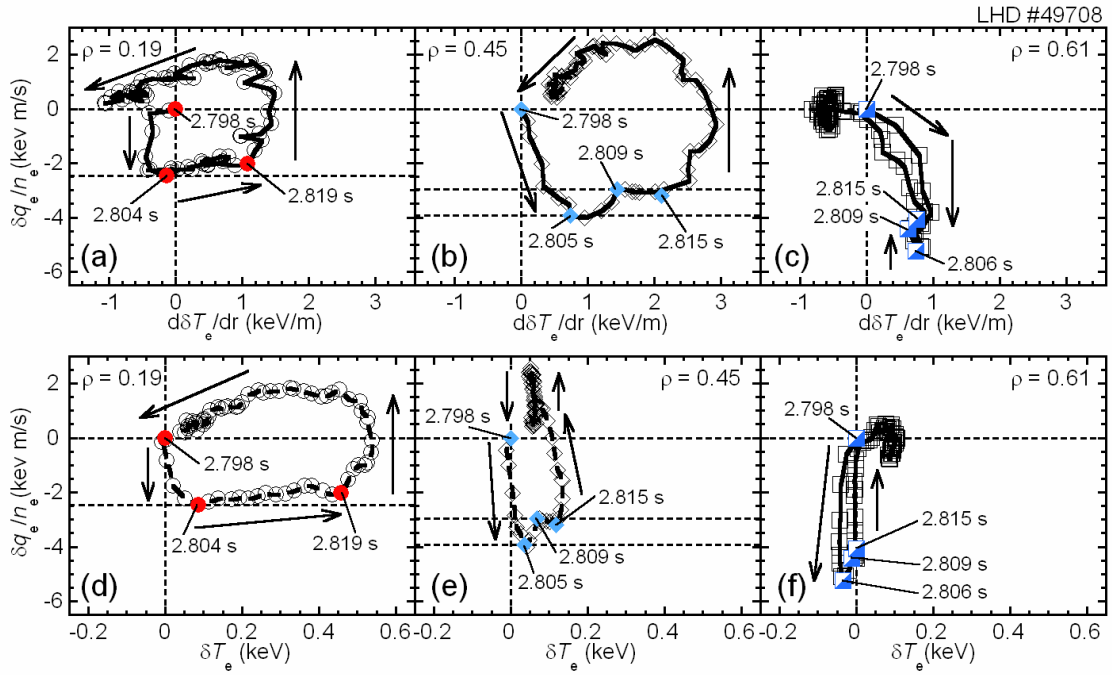

FIG. 5. The relation of the electron heat flux perturbation normalized by the electron density to (a, b, c) the gradient of the electron temperature perturbation and (d, e, f) the electron temperature perturbation at three different normalized minor radii. Each data point is obtained with an interval of 1 ms.

relations between the $\delta q_e/n_e$ versus the $\nabla\delta T_e$ and the $\delta q_e/n_e$ versus the δT_e at $\rho = 0.19$ and 0.45 show a hysteresis loop, while the relations at $\rho = 0.61$ does not shows a hysteresis loop. Even so, this trajectory is quite different from that based on the diffusive response. At $\rho = 0.19$, the reduction of the $\delta q_e/n_e$ just after the edge cooling is not accompanied by the appreciable change in local parameters, both the $\nabla\delta T_e$ and the δT_e (see FIGs 5(a) and 5(d)). Thus, in this phase, the electron heat transport at $\rho = 0.19$ is characterized by nondiffusive or nonlocal. When the larger TESPEL is injected into the plasma, in fact, the stronger edge cooling takes place, the decreasing rate of the $\delta q_e/n_e$ becomes higher. After the abrupt reduction of the $\delta q_e/n_e$, the $\nabla\delta T_e$ increases with the slight change in $\delta q_e/n_e$ from $t \sim 2.804$ s to $t \sim 2.819$ s. Thus the electron heat transport in this stage is characterized by the local process. It should be noted here that the turn-back of the $\delta q_e/n_e$ to the level before the edge cooling at $\rho = 0.19$ is not also accompanied by the change in both the $\nabla\delta T_e$ and the δT_e. Thus the transport governing this turn-back of the $\delta q_e/n_e$ at $\rho = 0.19$ can be also characterized by the nonlocal, although the trigger of this turn-back of the $\delta q_e/n_e$ is quite far from clear. Finally the $\delta q_e/n_e$ goes back to the preinjection level on the basis of local transport. At $\rho = 0.45$, the dynamic behavior of the data points in the space of the $\delta q_e/n_e$ versus the $\nabla\delta T_e$ is almost same as that at $\rho = 0.19$, except the presence of the metastable level in the $\delta q_e/n_e$. Regarding the relation between the $\delta q_e/n_e$ versus the δT_e, the variation of the $\delta q_e/n_e$ is not almost accompanied by that of the δT_e. At $\rho = 0.61$, the very initial behavior (within several milliseconds just after the TESPEL injection) of the $\delta q_e/n_e$ is accompanied by the change in both $\nabla\delta T_e$ and δT_e. And then the nonlocal characteristics appear strongly, while the diffusive characteristics appear in the transport at $\rho = 0.19$ and 0.45. These results suggest that the nonlocality of electron heat transport in the reduction phase of $\delta q_e/n_e$ appears first in the core region and secondly in the edge region, and that in the turn-back phase of $\delta q_e/n_e$ to the level before the edge cooling does first in the edge region and secondly in the core region.

Figure 6 shows the temporal evolutions of autoscaled $\delta q_e/n_e$ data at different normalized minor radii. In FIG. 6, the data points obtained with an interval of 1 ms are started from $t = 2.798$ s, same as those in FIG. 5. Just after the TESPEL injection, the $\delta q_e/n_e$ in the edge region ($\rho > 0.6$) increases abruptly, where the temperature decreases due to the process of the ablation and ionization of the TESPEL and the resulting cold pulse propagation. Shortly thereafter, the $\delta q_e/n_e$ in the outer region of the plasma ($\rho > 0.4$) decreases, followed by the $\delta q_e/n_e$ in the core region ($\rho < 0.4$) (see arrow A, indicated in FIG. 6). The decrease rate of the $\delta q_e/n_e$ at $\rho = 0.7$ is much higher than that in other regions. Thus this suggests that the behavior of the edge plasma is important to understand the nonlocal T_e rise. The termination of the decrease in $\delta q_e/n_e$ seems to propagate from the core to the edge (see arrow B). In the outer region with $\rho > 0.2$, the decrease in $\delta q_e/n_e$ seems to be overshot, and goes back to a metastable level. This rebound of the $\delta q_e/n_e$ to the metastable stage

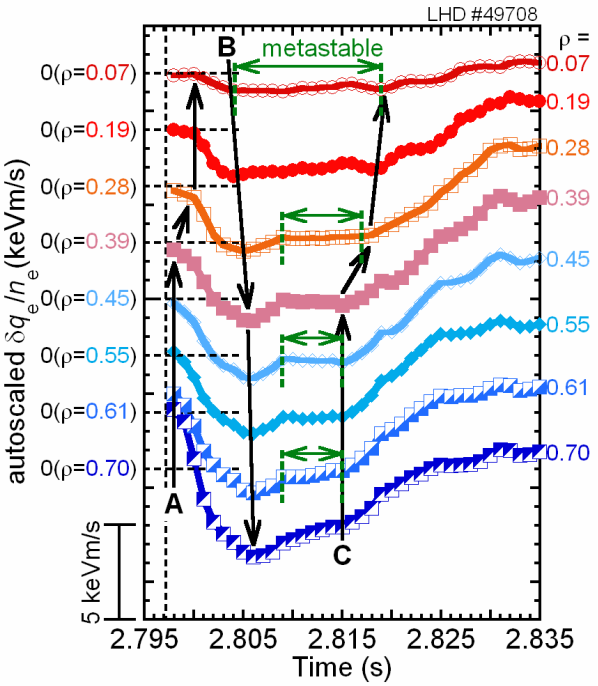

FIG. 6. Temporal evolutions of autoscaled electron heat flux perturbation normalized by the electron density data at different normalized minor radii. Each data point is plotted at 1 ms intervals. The TESPEL injection time is indicated as the vertical dashed line.

in the outer region is stopped almost simultaneously at $t \sim 2.089$ s. It should be noted here that, at $t \sim 2.815$ s, the turn-back of the $\delta q_e/n_e$ to the level before the edge cooling is started almost simultaneously (appreciable outside $\rho > 0.3$). This turn-back seems to propagate from the edge to the core (see arrow C). The time scale of the turn-back of the $\delta q_e/n_e$ to the level before the edge cooling is much slower than that of the first reduction of the $\delta q_e/n_e$. Therefore the transient response analysis for the nonlocal T_e rise clearly indicates the importance of the interaction between core and edge.

5. Discussion

Theoretical studies for the nonlocal response of the electron heat transport suggest the importance of the interaction of turbulence over long distance (nonlocality of the turbulence), such as turbulence spreading [14]. Microturbulence theory predicts two candidates for the electron transport, the ETG modes and the TEM modes. Based on a simple mixing length estimate, an ETG driven electron thermal diffusivity is generally much lower than an ITG/TEM driven one, except only when radially highly elongated vortices, so-called streamers, appear [15]. Thus the ETG turbulence might be ruled out as a candidate for the nonlocal T_e rise. The nonlocal T_e rise observed in the ECH plasma, which has the weakly driven ion heat channel, may suggest that ITG turbulence also could be ruled out. The TEM modes, which are generally coupled to the ITG modes, has some distinguishing features: those are stabilized in high collisionality regimes [16] and have a dependence on the electron density gradient scale length, magnetic shear and safety factor [17]. The nonlocal T_e rise in the LHD shows a dependence on the collisionality in the core region and the electron temperature gradient scale length in the edge region, as shown in FIG. 4. These results seem to show a positive relationship between the nonlocal T_e rise and the TEM turbulence. However, the role of the TEM modes in electron heat transport in the LHD is not exactly the same as in tokamaks. (The transient heat diffusivity χ_e^{tr} is larger than the χ_e^{PB} in tokamaks, on the other hand, the χ_e^{tr} is almost equal to the χ_e^{PB} in the LHD [4].) Moreover, there is no evidence that the electron density fluctuation, which is measured with the X-mode reflectometer, in the edge region is reduced in the vicinity of the nonlocal T_e rise. The results in the LHD indicate that the scale separation, neglecting fluctuations with other scale length, may be unreasonable for rationalizing the nonlocal T_e rise. In recent theoretical studies regarding plasma turbulence, nonlinear interactions between the different scale length modes is considered to be important [18]. Thus further experimental investigations are needed to clarify the relation between the nonlocal T_e rise and the plasma turbulence.

6. Summary

The core T_{e} rise in response to the rapid edge cooling is observed in the high temperature plasmas of LHD heliotron as well as tokamaks. The delay of the onset of the core T_{e} rise, which appears with the increase of electron density, is increased with the increase in the collisionality ν_b^* of the core plasma and the decrease in the electron temperature gradient scale length in the outer region of the plasma. The transient response analysis reveals that just after the edge cooling, the electron heat flux in the core region is decreased without change in local electron temperature and its gradient, thus, the core T_e rise invoked by the edge cooling is attributed to the nonlocality in the electron heat transport. The nonlocality of the electron heat transport in the reduction phase of electron heat flux perturbation normalized by the electron density appears first in the core region and secondly in the edge region, and that in the turn-back phase of electron heat flux perturbation normalized by the electron density to the level before the edge cooling does first in the edge region and secondly in the core region.

Acknowledgement

The authors acknowledge all of the technical staff of NIFS for their excellent support. They also would like to thank Prof. O. Motojima (Director of NIFS) for his continuous encouragement. This work is partly supported by a Grant-in-Aid for Scientific Research (B) (No. 15340201) from Japan Society for the Promotion of Science, a Grant-in-Aid for Young Scientists (B) (No. 17740372) from MEXT Japan and a budgetary Grant-in-Aid No.NIFS05ULHH510 of the National Institute for Fusion Science.

References

[1] CARDOZO, N. J. L., "Perturbative transport studies in fusion plasmas", Plasmas Phys. Controlled Fusion **37** (1995) 799.
[2] JACCHIA, A., et al., "Nonlinear perturbative electron heat transport study in the ASDEX Upgrade tokamak", Nucl. Fusion **45** (2005) 40.
[3] STROTH, U., et al., "Fast transport changes and power degradation in the W7-AS stellarator", Plasmas Phys. Controlled Fusion **38** (1996) 611.
[4] INAGAKI, S. et al, "Comparison of transient electron heat transport in LHD helical and JT-60U tokamak plasmas", Nucl. Fusion **46** (2006) 133.
[5] CALLEN, J. D., et al., "Evidence and concepts for non-local transport", Plasma Phys. Control. Fusion **39** (1997) B173.
[6] KINSEY, J. E. et al., "Theoretical transport modeling of Ohmic cold pulse experiments", Phys. Plasmas **5** (1998) 3974.
[7] TAMURA, N., et al., "Observation of core electron temperature rise in response to an edge cooling in toroidal helical plasmas", Phys. Plasma **12** (2005) 110705.
[8] YAMADA, H., et al., "Impact of heat deposition profile on global confinement of NBI heated plasmas in the LHD", Nuchl. Fusion **43** (2003) 749.
[9] SUDO, S., et al., "Diagnostics of Particle Transport by Double-Layer Pellet", J. Plasma Fusion Res. **69** (1993) 1349.
[10] INAGAKI, S., et al., "Observation of Reduced Heat Transport inside the Magnetic Island O Point in the Large Helical Device", Phys. Rev. Lett. **92** (2004) 055002.
[11] GALLI, P. et al, "`Non-local' response of RTP ohmic plasmas to peripheral perturbations", Nucl. Fusion **39** (1999) 1355.
[12] WALTER, H., et al., "Transient transport phenomena induced by cold pulses in W7-AS", Plasma Phys. Controlled Fusion **40** (1998) 1661.
[13] TANAKA, K., et al., "Experimental study of particle transport and density fluctuations in LHD", Nucl. Fusion **46** (2006) 110.
[14] HAHM, T. S., et al., "Turbulence spreading into the linearly stable zone and transport scaling", Plasma Phys. Control. Fusion **46** (2004) A323.
[15] JENKO, F., et al., "Electron temperature gradient driven turbulence", Phys. Plasmas **7** (2000) 1904.
[16] ANGIONI, C., et al., "Theory-based modeling of particle transport in ASDEX Upgrade H-mode plasmas, density peaking, anomalous pinch and collisionality", Phys. Plasmas **10** (2003) 3225.
[17] PEETERS, A. G., et al., "Linear gyrokinetic stability calculations of electron heat dominated plasmas in ASDEX Upgrade", Phys. Plasmas **12** (2005) 022505.
[18] ITOH, K. et a., "On transition in plasma turbulence with multiple scale lengths", Plasma Phys. Control. Fusion **45** (2003) 911.